Malays. Appl. Biol. (2017) 46(1): 171–175

SYNTHESIS OF A NANOPARTICLE SYSTEM FOR THE ENHANCED ACCUMULATION OF FLUORESCENTLY-LABELLED AMINO ACIDS ENCAPSULATED IN MONODISPERSED CHITOSAN NANOPARTICLE SYSTEM

UMMU AFIQAH HASSAN[1*], MOHD ZOBIR HUSSEIN[2] and MAS JAFFRI MASARUDIN[1]

[1]*Department of Cell and Molecular Biology, Faculty of Biotechnology and Biomolecular Sciences, Universiti Putra Malaysia, 43400 UPM Serdang, Selangor*
[2]*Institute of Advanced Technology, Universiti Putra Malaysia, 43400 UPM Serdang, Selangor*
[*]*E-mail: afiqah_289@yahoo.com*

Accepted 2 February 2017, Published online 31 March 2017

ABSTRACT

Poor *in vivo* bioavailability of nutrient is a major challenge in efficient delivery of nutraceutics. The increased bioavailability of nutraceuticals is prerequisite for efficient absorption by the gastrointestinal system. Nanotechnology-based approaches for nutraceutical applications could potentially increase absorption of nutrients and enhance its cellular accumulation due to its nanosize and promote better *in vivo* energy biodistribution. However, the dynamics of intracellular cell trafficking of nanoparticles and nutraceutical release has remain scarcely studied. This study describes a non-efficacious nanoparticle-mediated system for the encapsulation and delivery of fluorescently-labelled amino acids using tripolyphosphate as a crosslinker. Light scattering data showed successful formation of particle size as small as 65.69 nm with low polydispersity index (PDI) value of 0.178 at specific volume ratios of chitosan to tripolyphosphate. Following encapsulation, nanoparticle size and PDI value increased to 182.73 nm and 0.257 respectively discern successful accommodation of the fluorescently-labelled amino acid within its core. *In vitro* visualization of amino acids release and accumulation via fluorescence microscopy suggested that encapsulated amino acids were efficiently accumulated into Vero3 cell cytoplasm at 24 hours post treatment with localization in proximity to the cell nucleus. These results therefore suggested that the chitosan nanoparticle system developed was able to enhance the intracellular accumulation of glutamic acids and may serve as a suitable carrier for nutraceuticals delivery.

Key words: nutraceuticals, chitosan nanoparticles, nanobiotechnology, amino acid, bioavailability

INTRODUCTION

Recently, there has been an exponential interest in the development of nanotechnology-based delivery carriers for anticancer drugs (Mazzaferro *et al.*, 2013), proteins and peptides (Gupta *et al.*, 2013). Effective oral delivery of these therapeutic molecules is desirable but often challenging owing to the many physical and physiological barrier imposed primarily by the gastrointestinal track (GIT) system leading to poor biological efficacy and bioavailability (Bowman & Leong, 2006). This limitation hence has brought to the rapid onset on nanocarrier development towards improving their therapeutic efficacy, where chitosan nanoparticles have gained much attention owing to its special physiochemical features. Owing to its special physiochemical features such as low toxicity, high biodegradability and biocompatibility, chitosan has received a great traction in medical and biological researches (Nadarajah *et al.*, 2006). Chitosan is reported to act as a permeation enhancer by facilitating drug cellular uptake (Bowman & Leong, 2006) and its inherent mucoadhesive properties promote drug absorption thus increase drug cellular concentration and accumulation (Soane *et al.*, 1999). Over the past few years, bioactive compounds derived from plant origins and herbs are extensively used to treat common ailment and attributed as a potent adjuvant for some chronic diseases (Gianfrilli *et al.*, 2012). In spite of their known potential to provide added physiological and health benefits, the low *in vivo* bioavailability of nutraceutics limits their therapeutic applications (McClements & Li, 2010). The increased bioavailability of functional food ingredients such as amino acids is

* To whom correspondence should be addressed.

prerequisite for efficient absorption by GIT system. Nanotechnology-based approaches for nutraceutical applications could enhance the absorption of nutrients by the digestive systems and increase nutrients cellular accumulation as well. However, the studies on mechanism of nutraceutics as well as drug release and accumulation from nanocarriers are remain limited. Release studies would provide better elucidation on where and when nutraceutics are released from nanocarriers. It is important to track the release and localization of nutraceutics since most therapeutic compounds need to be internalized into cellular compartment and must achieve certain concentration to exert their therapeutic effects. This study proposes the synthesis of a chitosan-based nanoparticle system and elucidation of this system as a potential delivery carrier towards increasing *in vitro* cellular accumulation and localization of amino acids.

MATERIALS AND METHODS

Materials

Chitosan (low molecular weight), sodium tripolyphosphate (TPP), L-glutamic acid (GA), fluorescein 5(6)-isothiocyanate (FITC) and 4, 6-diamidino-2, phenylindole dihydrochloride (DAPI) in powder form were purchased from Sigma-Aldrich (St Louis, MO, USA). RPMI media 1640, 0.25% trypsin-EDTA and fetal bovine serum were purchased from Gibco, Life Technologies (Grand Island, USA). Sodium hydroxide pellet, 37% hydrochloric acid and acetic acid glacial were obtained from Friendmann Schmidt Chemicals (Germany).

Synthesis of chitosan nanoparticles (CNPs)

CNPs were synthesized by ionic gelation routes adapted and modified from Calvo *et al* (1997). Chitosan (CS) was firstly prepared at concentration of 1mg/mL. The CS was further diluted into 0.5 mg/mL final concentration an adjusted to pH 5. Separately, TPP solution was prepared at concentration of 1 mg/mL, and was then diluted into 0.7 mg/mL. The resulting TPP solutions were then adjusted to pH 2. CNPs were synthesized by mixing 600 µL CS solution into increasing volume of TPP solution (20 µL-300 µL). The resulting CNPs were then purified by centrifugation at 13 000 rpm for 20 minutes. The 40% of CNPs containing supernatant were then collected and diluted with 60% deionized distilled water and was used for further analysis and experimentation.

Synthesis of FITC-labelled GA (FITC-GA) encapsulated CNPs

GA solution was prepared by dispersing 0.086 mg GA powder in 10 mL deionized distilled water at 80ºC. The GA solution was subsequently diluted into 0.05 M final concentration. FITC was used as a labelling marker to tag GA. Briefly, 50 µL of FITC was added to 200 µL GA and incubated for 10 minutes in the dark. Incorporation of FITC-GA into CNP was achieved by adding the mixture of FITC-GA into 600 µL CS solution (0.5 mg/mL) prior addition of 250 µL of TPP (0.7 mg/mL). The mixture was then thoroughly mixed to ensure a homogenous suspension is obtained.

Analysis of CNP size and distribution by Dynamic Light Scattering (DLS)

The size and distribution of synthesized CNPs and FITC-GA encapsulated CNPs were analyzed by Dynamic Light Scattering using Malvern Zetasizer Nano S Instrument (Malvern Instruments, UK). The CNPs liquid suspension was directly loaded into a cuvette and the measurement of the particle size and distribution was performed in triplicate for each sample. Data are expressed as mean ± standard error of mean (SEM). Any significant difference of particle sizes between CNP samples prepared at different TPP volume was analyzed by One Way Analysis of Variance (ANOVA) whilst the significant difference of particle size preceding and following encapsulation was measured by paired *t*-test. The p value < 0.05 is considered as significant.

In vitro visualization of GA release and accumulation

FITC-GA encapsulated CNPs were prepared following steps described earlier. Vero3 kidney normal cells were seeded into 6 well plates at density of 0.8 $x10^5$ cells/well and was incubated for 24 hours. On the next day, cells were treated with 200 µL of the samples and were incubated for 6 hours and 24 hours. Prior to the visualization, the media from each well was discarded and the cells were washed once with 1X PBS. Approximately, 2mL of 4% formaldehyde was added into each well and was incubated for 3-5 minutes. The formaldehyde was then directly discarded and the cells were washed twice with 1X PBS. A volume of 2mL of DAPI solution was added to each well. The cells were then further incubated for 5 minutes. Following incubation, the DAPI was discarded and the cells were washed thrice with 1X PBS before new media was added. The release and accumulation of glutamic acids were observed under fluorescence microscopy.

RESULTS AND DISCUSSION

Particle size and distribution analyses by DLS

Formation of CNPs was mediated through electrostatic interaction between protonated amine groups of CS and anionic phosphate group of TPP (Shu & Zhu, 2002). Figure 1 shows the particles size produced at different TPP volume. The smallest CNP sizes (65.69±4.86 nm) were produced at 250 µL TPP addition to CS. The lowest PDI value of 0.178 (Figure 2) were also produced at this 250 µL TPP volume. The significant differences of particle sizes and PDI values were observed between CNPs prepared at 20 µL and 200 µL TPP, 20 µL and 250 µL TPP, 250 µL and 300 µL TPP as shown in Figure 1 and Figure 2. PDI value reflects how monodispersed the sample is and it is an indicator of particle stability and distribution (Lim *et al.*, 2013). As shown in Figure 1 and Figure 2, the CNP size and PDI value decreased as more TPP volume is added to CS. The gradual decreases in particle sizes were consistent with the increased availability of anionic TPP site. Upon addition of TPP to CS, protonated amine groups of CS start to crosslink with TPP to form CNPs and the crosslinking density is enhanced with further incorporation of TPP anion (Liu & Gao, 2009). However, above 250 µL of TPP addition, the particle size and PDI value increased to 169.43±1.72 nm and 0.257, respectively. At this point, only few free protonated amine groups of CS are accessible by TPP anion (Ravikumara & Madhusudhan, 2011). Further addition of TPP may

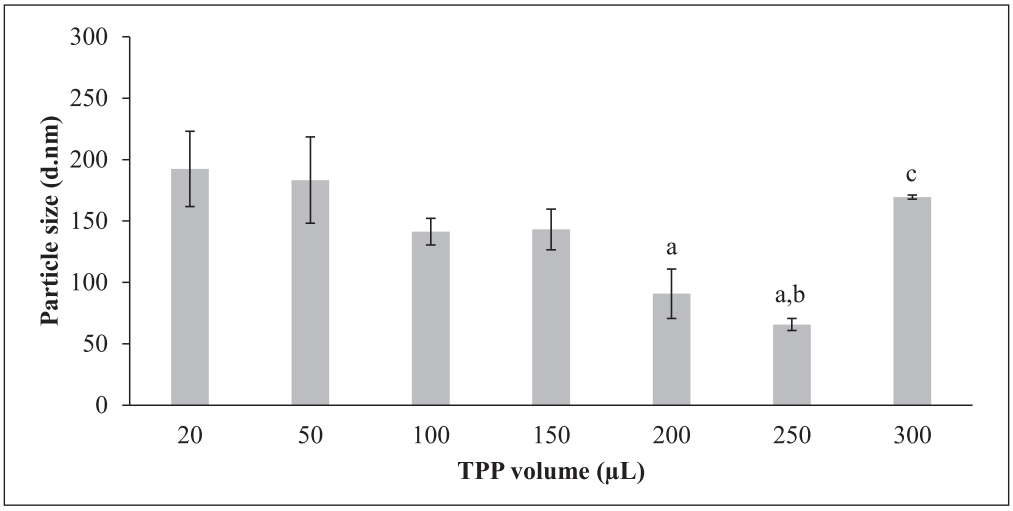

Fig. 1. Influence of TPP volume on particle size.

Notes: The particle size decreased with increasing TPP addition. The smallest particle size was produced at 250 µL TPP volume. Error bars represent SEM from triplicate independent experiment.
[a]Significant difference compared to 20 µL TPP addition. [b]Significant difference compared to 50 µL TPP addition. [c]Significant difference compared to 250 µL TPP addition.

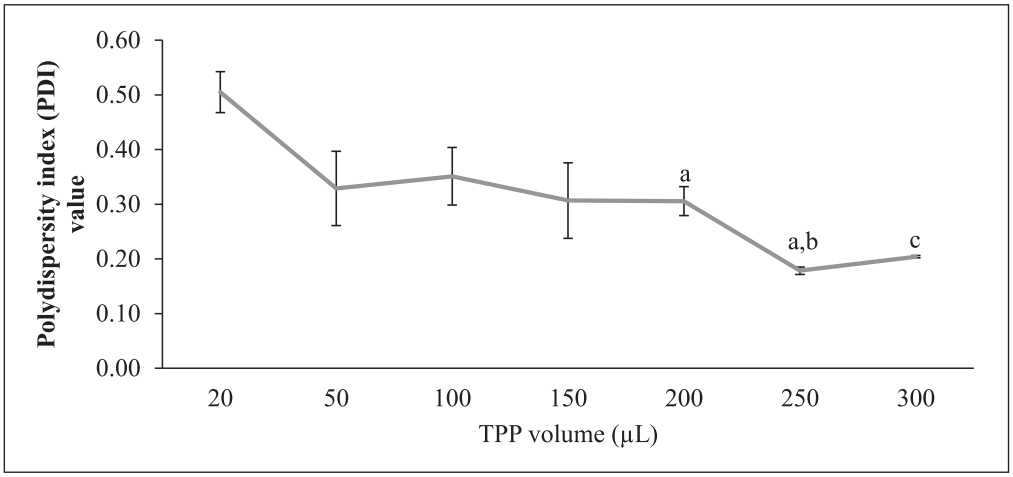

Fig. 2. Influence of TPP volume on PDI value.

Notes: The PDI value decreased with increasing TPP addition. The smallest PDI value was produced at 250 µL TPP volume. Error bars represent SEM from triplicate independent experiment.
[a]Significant difference compared to 20 µL TPP addition. [b]Significant difference compared to 50 µL TPP addition. [c]Significant difference compared to 250 µL TPP addition.

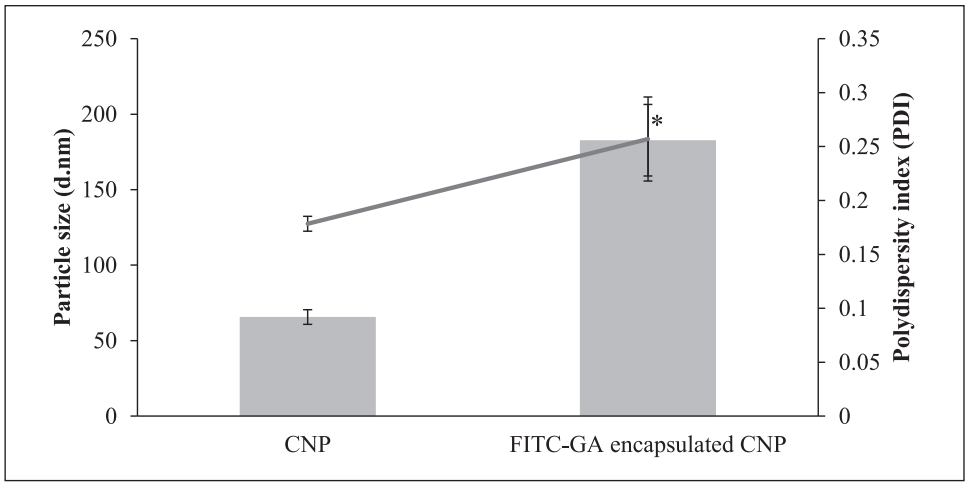

Fig. 3. Particle size and PDI value of CNP before and following FITC-GA encapsulation.
Notes: The particle size and PDI value increased following encapsulation. Error bars represent SEM from triplicate independent experiment.
*Significant difference of particle size of FITC-GA encapsulated CNP from CNP.

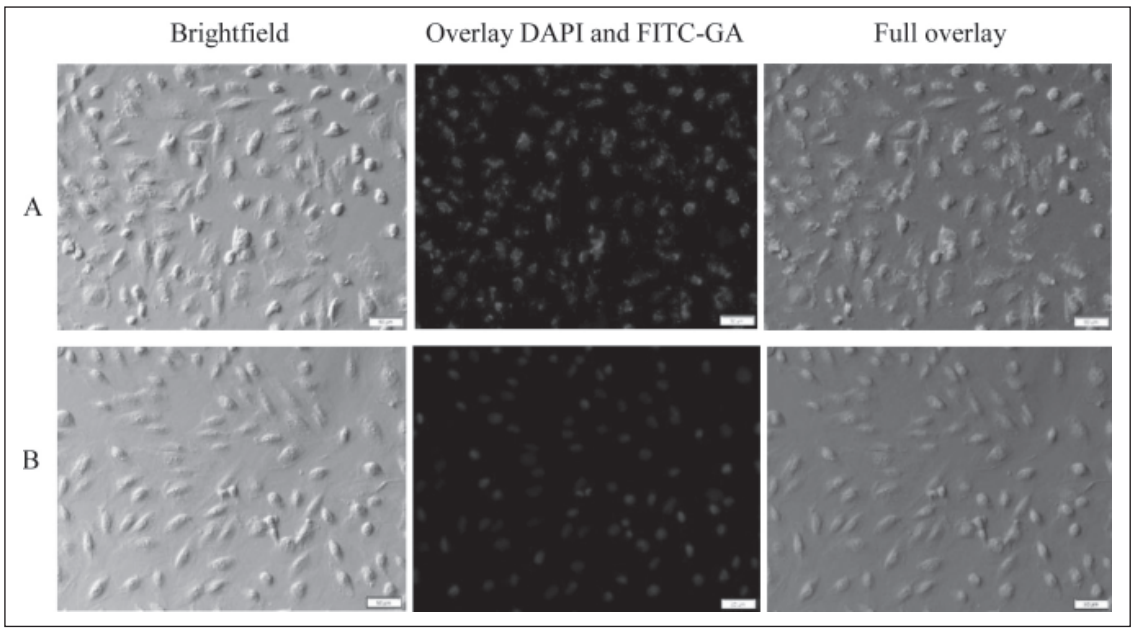

Fig. 4. *In vitro* cellular accumulation of FITC-GA (green) from CNPs into Vero3 cells.
Notes: Cells were treated with (A) FITC-GA encapsulated CNP for 24 hours and (B) free FITC- GA. DAPI was used to stain the cell nucleus (blue). No green fluorescence signal was observed for cells treated with free FITC-GA.

disrupt the ionic linkages of already formed CNPs which leads to formation of larger hydrodynamic particle size (Fan *et al*., 2012), thus explaining the increase in particle size and PDI value above 250 µL of TPP addition. These findings suggest that CNPs with small size and low PDI value were achieved at specific volume ratio of chitosan to TPP.

Figure 3 shows the size and PDI value of CNP preceding and following encapsulation. The bar graph and line graph represent CNP size and PDI value respectively. The CNP size increased from 65.69±4.86 nm to 182.73±23.73 following incorporation of FITC-GA into CNP. The increase in particles size postulates successful loading of FITC-GA within CNP. Encapsulation of FITC-GA increased PDI value from 0.178 to 0.257. This increase indicated the non-uniform distribution of CNP. The CNP population constituted broad ranges of particle size which consisted of free CNPs (< 100 nm) and FITC-GA encapsulated CNPs (> 100 nm).

In vitro accumulation of FITC-GA using fluorescence microscopy

In order to test the potential of the synthesized CNP system towards enhancing efficient accumulation of GA into cells, the GA were tagged with FITC. As shown in Figure 4A, fluorescence signal was detected in cells treated with FITC-GA

encapsulated CNPs. FITC-GA appears to accumulate in cell cytoplasm and some of it resides in close proximity to cell nucleus, while no fluorescence signal was observed in cells treated with free FITC-GA (Figure 4B). FITC-GA was found to only accumulate in cells when incorporated within the CNP carrier. No green fluorescence signal was detected in cells treated with free FITC-GA indicating that physical encapsulation within the CNP is pivotal for efficient accumulation of GA into cells. It was reported that encapsulation of molecules into nanocarrier would enhance their internalization into cells compared to free dosage form (Alexis *et al.*, 2008).

CONCLUSION

The formation of small, monodispersed CNP size was achieved at specific volume ratio of CS to TPP. The nanoparticle size increased following encapsulation of FITC-GA indicates the successful accommodation of the molecules within CNP core. Visualization of FITC-labeled GA release and accumulation from CNP system suggests the potential of this CNP system towards enhancing intracellular accumulation of GA thus may serve as a potential carrier for food ingredients in nutraceutical field as well as drug delivery of protein and peptides for medical applications.

ACKNOWLEDGEMENTS

The author UAH would like to thank the Ministry of Education, Malaysia for the myBrain15 scholarship, and Universiti Putra Malaysia for provisions of a Graduate Research Fellowship. The author MJM would like to acknowledge Universiti Putra Malaysia for research funding under the *Inisiatif Putra Muda* (IPM) scheme.

REFERENCES

Alexis, F., Pridgen, E., Molnar, L.K. & Farokhzad, O.C. 2008. Factors affecting the clearance and biodistribution of polymeric nanoparticles. *Molecular Pharmaceutics*, **5(4):** 505-515.

Bowman, K. & Leong, K.W. 2006. Chitosan nanoparticles for oral drug and gene delivery. *International Journal of Nanomedicine*, **1(2)**: 117.

Calvo, P., RemunanLopez, C., VilaJato, J.L. & Alonso, M.J. 1997. Novel hydrophilic chitosan-polyethylene oxide nanoparticles as protein carriers. *Journal of Applied Polymer Science,* **63(1):** 125-132.

Fan, W., Yan, W., Xu, Z. & Ni, H. 2012. Formation mechanism of monodisperse, low molecular weight chitosan nanoparticles by ionic gelation technique. *Colloids and Surfaces B: Biointerfaces*, **90:** 21-27.

Gianfrilli, D., Lauretta, R., Di Dato, C., Graziadio, C., Pozza, C., De Larichaudy, J., Giannetta, E., Isidori, A.M. & Lenzi, A. 2012. Propionyl-L-carnitine, Larginine and niacin in sexual medicine: a nutraceutical approach to erectile dysfunction. *Andrologia*, **44(s1):** 600-604.

Gupta, S., Jain, A., Chakraborty, M., Sahni, J.K., Ali, J. & Dang, S. 2013. Oral delivery of therapeutic proteins and peptides: a review on recent developments. *Drug Delivery*, **20(6):** 237-246.

Lim, J., Yeap, S.P., Che, H.X. & Low, S.C. 2013. Characterization of magnetic nanoparticle by dynamic light scattering. *Nanoscale Research Letters*, **8(1):** 1-14.

Liu, H. & Gao, C. 2009. Preparation and properties of ionically crosslinked chitosan nanoparticles. *Polymers for Advanced Technologies*, **20(7):** 613-619.

Mazzaferro, S., Bouchemal, K. & Ponchel, G. 2013. Oral delivery of anticancer drugs III: formulation using drug delivery systems. *Drug Discovery Today*, **18(1):** 99-104.

McClements, D.J. & Li, Y. 2010. Review of *in vitro* digestion models for rapid screening of emulsion-based systems. *Food & Function,* **1(1),** 32-35.

Nadarajah, K., Lau, B.Y.C., Othman, O., Hasidah, M.S. & Wan-Mohtar, W.Y. (2006). Characterization of chitin deacetylase from fungus *Absidia butleri dr. Malaysian Applied Biology*, **35(2)**: 59.

Ravikumara, N.R. & Madhusudhan, B. 2011. Chitosan nanoparticles for tamoxifen delivery and cytotoxicity to MCF-7 and Vero cells. *Pure and Applied Chemistry*, **83(11):** 2027-2040.

Shu, X.Z. & Zhu, K.J. 2002. The influence of multivalent phosphate structure on the properties of ionically cross-linked chitosan films for controlled drug release. *European Journal of Pharmaceutics and Biopharmaceutics*, **54(2):** 235-243.

Soane, R.J., Frier, M., Perkins, A.C., Jones, N.S., Davis, S.S. & Illum, L. 1999. Evaluation of the clearance characteristics of bioadhesive systems in humans. *International Journal of Pharmaceutics*, **178(1):** 55-65.